Comments on "Oscillatory Bottom Boundary Layers"

LAKSHMI H. KANTHA

Department of Aerospace Engineering Sciences, University of Colorado, Boulder, Colorado

(Manuscript received 2 August 2004, in final form 2 August 2004)

1. Introduction

Bottom boundary layers in shallow waters on the inner continental shelf are invariably under the influence of propagating surface gravity waves. Wave-induced oscillatory currents superimposed on the mean current alter the velocity profile in the water column and increase the roughness felt by the mean current. The apparent roughness z_{0a} is given by

$$\frac{z_{0a}}{z_0} = 1 + F\left(\frac{u_b}{u_{*c}}, \frac{A_b}{k_s}, \varphi\right), \tag{1}$$

where z_0 is the roughness scale without wave-induced currents, u_b is the magnitude of the wave-induced bottom current, u_{*c} is the mean friction velocity due to the mean current, $k_s = 30z_0$ is the Nikuradse equivalent roughness, φ is the angle between the mean current and wave propagation direction, and $A_b = u_b/\omega$, with ω being the wave frequency. Of the parameters that affect function *F,* the most important are u_b/u_{*c} and A_b/k_s; parameter φ has a somewhat weaker influence.

Mellor (2002, henceforth M02) has applied a second-moment closure-based turbulence model (Mellor and Yamada 1982) to oscillatory bottom boundary layers. He simulates a purely oscillatory boundary layer and demonstrates that the resulting numerical model velocity profiles compare reasonably well to the laboratory data of Jensen et al. (1989). He then applies the same method to oscillatory flows superimposed on a mean flow and plots z_{0a}/z_0 as a function of u_b/u_{*c} for various values of A/z_0. However, he does not compare his results with published data on apparent roughness. Instead, he compares them with the analytical results of Grant and Madsen (1979, 1986, henceforth GM) plotted the same way (his Fig. D1). He concludes that his curves are shifted to the right vis-à-vis GM curves. This of course means that for the same values of u_b/u_{*c} and A/z_0, M02 underestimates the increase in roughness due to wave-induced motions by roughly an order of magnitude. For example, for $u_b/u_{*c} = 20$ and $\varphi = 0$, M02 yields z_{0a}/z_0 ~3.4, whereas GM yields z_{0a}/z_0 ~69 for $z_0/A_b = 10^{-4}$. If z_0/A_b is decreased to 10^{-6}, M02 value is substantially unchanged while GM yields z_{0a}/z_0 ~693.

The study raises several questions. First, how do M02 results compare with published data? Does GM theory, the accepted standard for the past two decades, perform better? Is there anything that can be done to improve the agreement with data? This note is an attempt to answer these questions.

Considerable effort has gone into determining the form of function *F* in Eq. (1). Because it is hard to estimate z_0 from field experiments and hence z_{0a}/z_0, only laboratory experiments (Kemp and Simons 1982, 1983; Asano et al. 1986; van Doorn 1981, 1982; Sleath 1990) have provided a reliable means of estimating z_{0a}/z_0. Figure 1a shows z_{0a}/z_0 plotted against u_b/u_{*c}; Fig. 1b shows z_{0a}/z_0 plotted against $(u_b/u_{*c})(A_b/k_s)^{1/2}$.

Sleath (1991) has suggested the following empirical relationship:

$$\frac{z_{0a}}{z_0} = 1 + 0.19\left(\frac{u_b}{u_{*c}}\right)\sqrt{\frac{A_b}{k_s}}, \tag{2}$$

which is also shown plotted in Figs. 1a and 1b. It is evident that Eq. (2) is a reasonable fit to the data, which have A_b/k_s values ranging from 0.5 to over 100. Note, however, that when the waves propagate against the

Corresponding author address: Lakshmi H. Kantha, Department of Aerospace Engineering Sciences, CB 431, University of Colorado, Boulder, CO 80309.
E-mail: kantha@colorado.edu

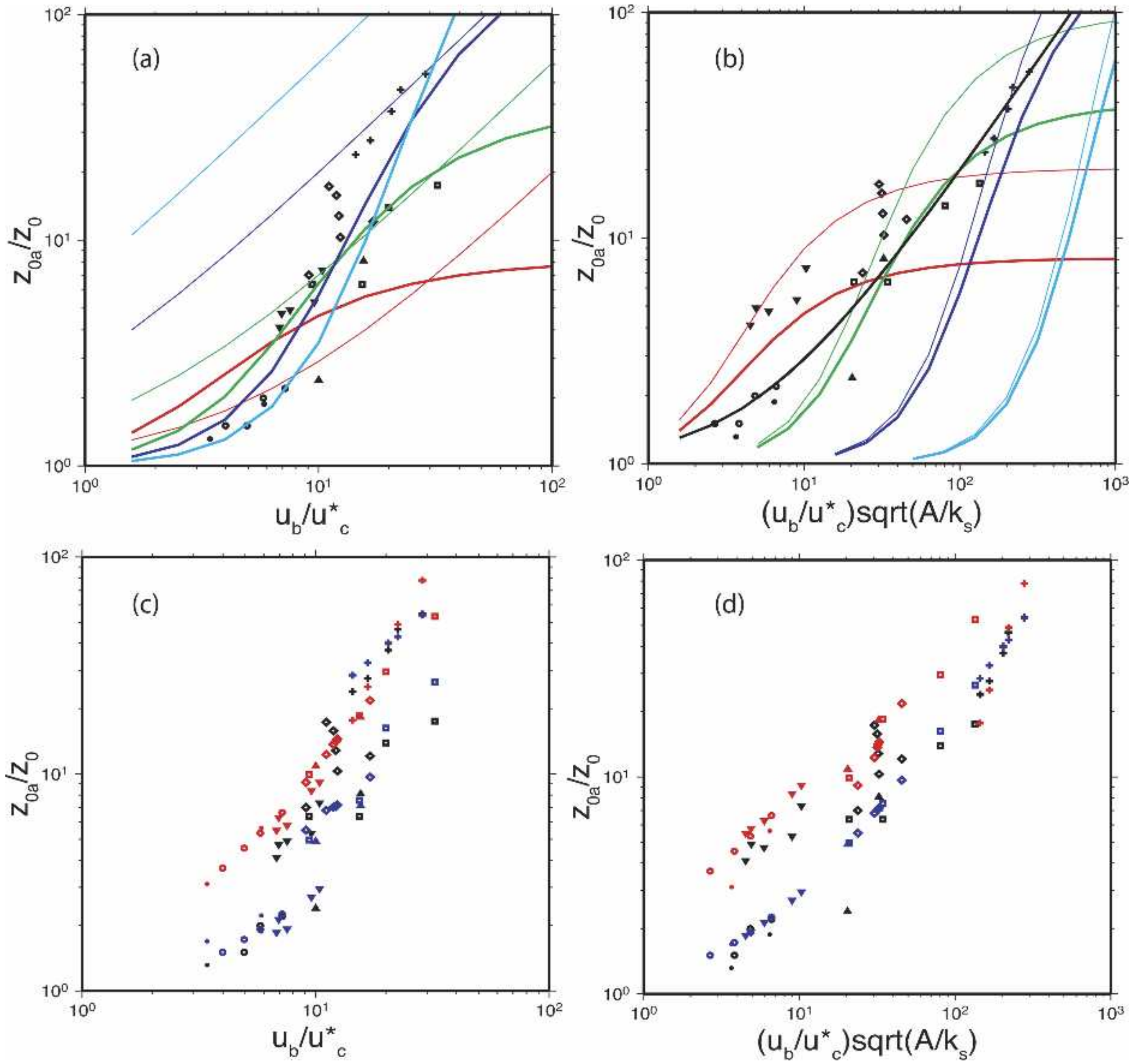

FIG. 1. (a) Plot of z_{0a}/z_0 against u_b/u_{*c}. Thick curves show Grant and Madsen (1986, hereinafter GM86) theoretical solutions [Eq. (7): $\varphi = 0$], and thin curves show Sleath (1991) values [Eq. (2)] for $A_b/k_s = 1$ (red), 10 (green), 100 (blue), and 1000 (light blue). Observational data points are shown in black: small circles show data for Asano et al. (1986; $\varphi = 0°$, $A_b/k_s \sim 1.14–1.21$), circles are from Kemp and Simons (1982; $\varphi = 0°$, $A_b/k_s \sim 0.45–0.85$), inverted triangles are from Kemp and Simons (1983; $\varphi = 180°$, $A_b/k_s \sim 0.42–0.98$), triangles are from van Doorn (1981; $\varphi = 0°$, $A_b/k_s \sim 4.2–4.3$), squares are from van Doorn (1982; $\varphi = 0°$, $A_b/k_s \sim 4.9–17.2$), diamonds are from Sleath (1990; $\varphi = 90°$, $A_b/k_s \sim 6.8–7.5$), and pluses are from Sleath (1990; $\varphi = 90°$, $A_b/k_s \sim 94–101$). The data are taken from Nielsen (1992). (b) Plot of z_{0a}/z_0 against $(u_b/u_{*c})(A_b/k_s)^{1/2}$. Thick (thin) curves show GM86 original (modified) theoretical solutions [Eq. (7): $\varphi = 0$] for $A_b/k_s = 1$ (red), 10 (green), 100 (blue), and 1000 (light blue). The black curve shows Sleath (1991) values [Eq. (2)]. The observational data points are as in (a). (c) Plot of z_{0a}/z_0 against u_b/u_{*c}. The observational data points are as in (a). Red points correspond to the modified GM theory, and blue points correspond to the Sleath law for the same values of A_b/k_s and u_b/u_{*c} as the observational data points. (d) Plot of z_{0a}/z_0 against $(u_b/u_{*c})(A_b/k_s)^{1/2}$. Observational data points are as in (a). Red points correspond to the modified GM theory, and blue points correspond to the Sleath law for the same values of A_b/k_s and u_b/u_{*c} as the observational data points.

current ($\varphi = 180°$) the apparent roughness appears to be higher than when they propagate with the current ($\varphi = 0°$) (see Kemp and Simons 1982, 1983) and the data points for $\varphi = 180°$ (inverted triangles) fall significantly above the Sleath curve in Fig. 1b. Nevertheless, the Sleath empirical law Eq. (2) provides a decent fit to the available experimental data. For a typical 12-s swell of 15-cm amplitude propagating through a region with a rough bottom ($z_0 = 1$ cm), $A_b/k_s \sim 0.5$. If $z_0 = 1$ mm, $A_b/k_s \sim 5$. Thus the values in the field are well within the range of these experiments. Note, however, that F does not go to zero as u_b/u_{*c} approaches zero and hence this law is invalid for the mean-current-only case.

The M02 studies were conducted only for A_b/k_s values of 333, 3333, and 33 333, which are well outside the range covered by the experimental data. As a consequence, it is impossible to compare his results with experimental data. The GM results can be, as is shown below.

2. Comparison of GM analytical results with data

M02 details the GM analytical approach for computing z_{0a}/z_0. We repeat it here for reasons that will be clear shortly.

When oscillatory motion due to waves is superimposed on the mean current, there exists a wave boundary layer embedded within the bottom boundary layer so that the mean velocity profile can be written as

$$u(z) = \frac{\tau_c}{\kappa u_{*cw}} \ln\left(\frac{z}{z_0}\right) \quad \text{for} \quad z \ll \delta_{cw} \quad \text{and}$$

$$u(z) = \frac{\tau_c}{\kappa u_{*c}} \ln\left(\frac{z}{z_{0a}}\right) \quad \text{for} \quad z \gg \delta_{cw}, \tag{3}$$

where z_0 is the physical roughness parameter and z_{0a} is the apparent roughness felt by the mean flow; τ_c is the shear stress, and δ_{cw} is the thickness of the wave boundary layer, assumed to be much smaller than the bottom boundary layer.

Matching the two velocities at $z = \delta_{cw}$ gives

$$\frac{z_{0a}}{z_0} = \left(\frac{\delta_{cw}}{z_0}\right)^{1-\varepsilon}; \ \varepsilon = \frac{u_{*c}}{u_{*cw}}; \tag{4}$$

GM assume

$$\delta_{cw} = \frac{2\kappa u_{*cw}}{\omega} \quad \text{and} \tag{5}$$

$$\frac{u_{*cw}^2}{u_b^2} = \frac{f_w}{2}\left[1 + 2\left(\frac{u_{*c}}{u_{*mw}}\right)^2 \cos\varphi + \left(\frac{u_{*c}}{u_{mw}}\right)^4\right]^{\frac{1}{2}};$$

$$u_{*mw}^2 = \frac{f_w}{2}u_b^2, \tag{6}$$

so that

$$\frac{z_{0a}}{z_0} = \left[60\kappa\left(\frac{A_b}{k_s}\right)\left(\frac{u_{*cw}}{u_b}\right)\right]^{1-\varepsilon}, \tag{7}$$

where

$$f_w = 0.23\left(\frac{A_b}{k_s}\right)^{-0.62} \quad \text{for} \quad \left(\frac{A_b}{k_s}\right) \le 12.5 \quad \text{and}$$

$$f_w = 0.13\left(\frac{A_b}{k_s}\right)^{-0.40} \quad \text{for} \quad \left(\frac{A_b}{k_s}\right) > 12.5. \tag{8}$$

Equations (4)–(8) must be solved by an iterative process. For $\varphi = 0°$, however, no iteration is necessary and one gets

$$\frac{z_{0a}}{z_0} = \left[60\kappa\left(\frac{A_b}{k_s}\right)\left(\frac{f_w}{2} + \frac{u_{*c}^2}{u_b^2}\right)^{1/2}\right]^{1-\varepsilon};$$

$$\varepsilon = \left(\frac{f_w}{2}\frac{u_b^2}{u_{*c}^2} + 1\right)^{-1/2}. \tag{9}$$

These are also plotted in both Figs. 1a and 1b. It is clear that GM theory as presented in M02 significantly underestimates the apparent roughness scale.

A very slight modification is sufficient to improve the agreement, however (see also Madsen and Wikramanayake 1991). Because there is no justification for including the von Kármán constant κ in Eq. (5), we propose that it be omitted so that Eq. (7) holds but without κ in the square brackets. As seen from Fig. 1b, this approach leads to some improvement in the agreement between GM theory and data. To demonstrate this further, we plot in Figs. 1c and 1d, the z_{0a}/z_0 values given by GM theory for the values of A_b/k_s and u_b/u_{*c} that correspond to observed data points. The points given by the Sleath law are also plotted. It is clear that the agreement between GM theory and the data is improved. Note also that the agreement between data and GM theory for $\varphi = 180°$ (inverted triangles) is better than that for the Sleath law. The agreement is by no means perfect, however. See Madsen (1994) and Mathisen and Madsen (1999) for more recent studies of the wave-current boundary layer.

3. Concluding remarks

It is noteworthy that for the same value of A_b/k_s, M02 estimates of apparent roughness are smaller than the values from even the original GM formulation, which, of course, underestimates the increase in apparent roughness relative to experimental data. The reason for this underestimate by M02 of the apparent roughness is not clear. It could be that the wave boundary layer within the bottom boundary layer was not resolved well. Also, M02 studies must be carried out for A_b/z_0 values of 15–3000 before a definitive statement can be made as to whether M02 produces results in substantial agreement with experimental data. It should be pointed out, however, that M02 results do agree well with Jensen et al. (1989) data for which $u_{*c} = 0$ and regular channel data for which $u_b = 0$.

Acknowledgments. The author thanks ONR and Dr. Manuel Fiadeiro for support for this work through ONR Grant N00014-03-1-0488.

REFERENCES

Asano, T., M. Nagakawa, and Y. Iwagaki, 1986: Changes in current profiles due to wave superimposition. *Proc. 20th Int. Conf. on Coastal Engineering,* Taipei, Taiwan, American Society of Civil Engineers, 925–940.

Grant, W. D., and O. S. Madsen, 1979: Combined wave and current interaction with a rough bottom. *J. Geophys. Res.,* **84,** 1797–1808.

——, and ——, 1986: The continental-shelf bottom boundary layer. *Annu. Rev. Fluid Mech.,* **18,** 265–305.

Jensen, B. L., B. M. Summer, and J. Fredsoe, 1989: Turbulent oscillatory boundary layers at high Reynolds numbers. *J. Fluid Mech.,* **206,** 265–297.

Kemp, P. H., and R. R. Simons, 1982: The interaction between waves and a turbulent current: Waves propagating with the current. *J. Fluid Mech.,* **116,** 227–250.

——, and ——, 1983: The interaction between waves and a turbulent current: Waves propagating against the current. *J. Fluid Mech.,* **130,** 73–89.

Madsen, O. S., 1994: Spectral wave-current bottom boundary layer flows. *Proc. 24th Int. Conf. on Coastal Engineering*, Vol. 1, Kobe, Japan, American Society of Civil Engineers, 384–398.

——, and P. N. Wikramanayake, 1991: Simple model for turbulent wave-current bottom boundary layer flow. Contract Rep. DRP-91-1, U.S. Army Corps of Engineers, Coastal Engineering Research Center, Vicksburg, MS, 125 pp.

Mathisen, P. P., and O. S. Madsen, 1999: Waves and currents over a fixed rippled bed 3. Bottom and apparent roughness for spectral waves and currents. *J. Geophys. Res.,* **104,** 19 447–19 461.

Mellor, G., 2002: Oscillatory bottom boundary layers. *J. Phys. Oceanogr.,* **32,** 3075–3088.

——, and T. Yamada, 1982: Development of a turbulence closure model for geophysical fluid problems. *Rev. Geophys. Space Phys.,* **20,** 851–875.

Nielsen, P., 1992: *Coastal Bottom Boundary Layers and Sediment Transport*. World Scientific, 324 pp.

Sleath, J. F. A., 1990: Bed friction and velocity distributions in combined steady and oscillatory flow. *Proc. 22d Int. Conf. on Coastal Engineering,* Delft, Netherlands, American Society of Civil Engineers, 450–463.

——, 1991: Velocities and shear stresses in wave-current flows. *J. Geophys. Res.,* **96,** 15 237–15 244.

van Doorn, T., 1981: Experimental investigation of near-bottom velocities in water waves without and with a current. TOW Rep. M 1423 Part 1, Delft Hydraulics Laboratory, 87 pp.

——, 1982: Experimental investigation of near-bottom velocities in water waves without and with a current. TOW Rep. M 1562-1a Part 1, Delft Hydraulics Laboratory.